Electrochimica Acta 55 (2010) 3055–3060

Contents lists available at ScienceDirect

Electrochimica Acta

journal homepage: www.elsevier.com/locate/electacta

# A novel hydrogen peroxide biosensor based on Au–graphene–HRP–chitosan biocomposites

Kangfu Zhou [a], Yihua Zhu [a,*], Xiaoling Yang [a], Jie Luo [a], Chunzhong Li [a], Shaorong Luan [b,*]

[a] Key Laboratory for Ultrafine Materials of Ministry of Education, School of Materials Science and Engineering, East China University of Science and Technology, 130 Meilong Road, Shanghai 200237, China
[b] Research Center of Analysis and Test, School of Chemistry and Molecular Engineering, East China University of Science and Technology, Shanghai 200237, China

ARTICLE INFO

*Article history:*
Received 10 October 2009
Received in revised form 8 January 2010
Accepted 11 January 2010
Available online 18 January 2010

*Keywords:*
$H_2O_2$ biosensor
Graphene
Au nanoparticles
Horseradish peroxidase
Electrocatalyze

ABSTRACT

Graphene was prepared successfully by introducing $-SO_3^-$ to separate the individual sheets. TEM, EDS and Raman spectroscopy were utilized to characterize the morphology and composition of graphene oxide and graphene. To construct the $H_2O_2$ biosensor, graphene and horseradish peroxidase (HRP) were co-immobilized into biocompatible polymer chitosan (CS), then a glassy carbon electrode (GCE) was modified by the biocomposite, followed by electrodeposition of Au nanoparticles on the surface to fabricate Au/graphene/HRP/CS/GCE. Cyclic voltammetry demonstrated that the direct electron transfer of HRP was realized, and the biosensor had an excellent performance in terms of electrocatalytic reduction towards $H_2O_2$. The biosensor showed high sensitivity and fast response upon the addition of $H_2O_2$, under the conditions of pH 6.5, potential −0.3 V. The time to reach the stable-state current was less than 3 s, and the linear range to $H_2O_2$ was from $5 \times 10^{-6}$ M to $5.13 \times 10^{-3}$ M with a detection limit of $1.7 \times 10^{-6}$ M (S/N = 3). Moreover, the biosensor exhibited good reproducibility and long-term stability.



## 1. Introduction

Graphene, which has been characterized as "the thinnest material in our universe" [1], has attracted a tremendous amount of attention because of a few intriguing attributes it displays. Graphene is a single layer of carbon atoms with a hexagonal arrangement in a two-dimensional lattice. It can be seen as the basic building block for graphitic materials. The unique properties of graphene include fast electron transportation, high thermal conductivity, excellent mechanical stiffness and good biocompatibility [2], which result in promising applications in nanocomposites [3], field-effect transistors [4], electromechanical resonators [5], solar cells [6] and electrochemical sensors [7,8].

On the other hand, the determination of hydrogen peroxide is of great importance in chemistry, biology [9,10], clinical control [11] and environmental protection [12]. Many techniques have been developed to detect hydrogen peroxide, including titrimetry [13], fluorimetry [14], spectrophotometry [15], chemiluminescence [16] and electrochemical sensors [17–19]. Among them, most involve high cost and are time consuming, except for electrochemical sensors. Due to their simplicity, high sensitivity and selectivity, electrochemical methods have been extensively employed in hydrogen peroxide determination. Carbon nanotubes (CNTs) have been widely used to fabricate electrochemical $H_2O_2$ biosensors due to their high electrical conductivity and excellent electrocatalytic activity towards $H_2O_2$. Zhang and co-workers successfully functionalized single-walled carbon nanotubes (SWCNTs) with one kind of electroactive inorganic compound: chromium hexacyanoferrate (Cr hcf). The nanocomposite-modified glassy carbon electrode showed high electrocatalytic activity towards the reduction of $H_2O_2$ [20]. Pillay and Ozoemena fabricated a nanostructured phthalocyaninatoiron(II)/SWCNT-poly(m-aminobenzenesulfonic acid) hybrid system on a gold surface using a layer-by-layer self-assembly strategy. The as-modified electrode displayed a significant amplification of the electrochemical response to $H_2O_2$ detection, suggesting that this CNTs-based electrode could provide an important nano-architectural sensing platform for the development of a sensor [21]. The successful utilization of carbon nanotubes as "molecular wires" has realized the direct electron transfer between redox centers of enzymes and electrodes, which leads to the new mediator-free biosensor [22–24]. Graphene, another carbon-based material, has shown several characteristics that may be very beneficial in designing electrochemical sensors, such as high surface area-to-volume ratio, fast electron transferring rate and good biocompatibility. Considering the convenient and low cost fabrication procedure, graphene is expected to be a perfect alternative electrode material to carbon nanotubes. Recently, Niu and co-workers [7] have

* Corresponding authors. Tel.: +86 21 64252022; fax: +86 21 64250624.
*E-mail addresses:* yhzhu@ecust.edu.cn (Y. Zhu), srluan@ecust.edu.cn (S. Luan).

0013-4686/$ – see front matter © 2010 Elsevier Ltd. All rights reserved.
doi:10.1016/j.electacta.2010.01.035

reported a novel glucose biosensor based on the combination of polyvinylpyrrolidone-protected graphene, polyethylenimine functional ionic liquid and glucose oxidase. This biosensor has achieved the direct electron transfer of glucose oxidase, maintained the bioactivity of the enzyme and showed excellent electrocatalysis towards glucose. These results demonstrate that graphene is an eximious electrode material and can enhance the performance of biosensors.

In this paper, we successfully utilized as-synthesized graphene to construct a novel $H_2O_2$ biosensor. Horseradish peroxidase (HRP) was selected as a model enzyme and immobilized in chitosan (CS). Possessing a number of attractive properties such as high permeability toward water, good adhesion, biocompatibility [25] and good film formation, the biopolymer chitosan is considered a suitable matrix for enzyme immobilization and is widely used in fabricating biosensors. Furthermore, chitosan is positively charged when pH < 6.3 due to the protonation of amino groups. Because our synthesized graphene is negatively charged due to the existence of sulfonic groups, the graphene could be well dispersed in chitosan solution via the Coulomb effect and formed a unique film on the surface of a glassy carbon electrode (GCE). We also introduced Au nanoparticles into the $H_2O_2$ biosensor due to their high surface-to-volume ratio, good biocompatibility, high catalytic efficiency and chemical stability [26]. It has been reported that the integration of carbon-based materials and metal nanoparticles liked CNT–Pt composites offers synergistic effects in electrocatalytic applications [27], so we have reasons to expect the graphene–Au composite has the same effect. Electrodeposition was employed to prepare the Au nanostructure film on the graphene/HRP/CS modified electrode because it is a simple and controllable method. The resulting biosensor exhibits excellent electrocatalytic response to $H_2O_2$, along with a wide linear range and long-term stability.

## 2. Experimental

### 2.1. Reagents and materials

HRP (from horseradish, 250 U/mg) and chitosan (medium molecular weight) were purchased from Sigma and used without further purification. Graphite powder and $HAuCl_4{\cdot}4H_2O$ were purchased from Sinopharm Chemical Reagent Co., Ltd. 30% $H_2O_2$ solution was purchased from Shanghai Lingfeng Chemical Reagent Co., Ltd, and a fresh solution of $H_2O_2$ was prepared daily. All other chemicals were of analytical grade and used as received. The 0.1 M phosphate buffer solutions (PBS) at various pH values were prepared by mixing the stock solutions of 0.1 M $NaH_2PO_4$ and 0.1 M $Na_2HPO_4$ with different proportion. The pure water (18 MΩ cm) used to prepare all solutions in this study was purified with a water system provided by Shanghai Winner Environmental Technology Co., LCD.

### 2.2. Apparatus

Electrochemical measurements were carried out with a CHI 660C workstation (CH Instruments, Chenhua, Shanghai, China) connected to a personal computer. A three-electrode configuration was employed, consisting of a modified glassy carbon electrode (3 mm in diameter) serving as the working electrode, and Ag/AgCl (3 M KCl) and platinum wire serving as the reference and counter electrodes respectively. All electrochemical experiments were carried out at room temperature, and all experimental solutions were degassed by nitrogen for at least 15 min. Then a nitrogen atmosphere was maintained during the electrochemical measurements.

The transmission electron microscope (TEM) and scanning electron microscope (SEM) images were obtained using a JEOL-2100F transmission electron microscope equipped with an INCA X-ray energy dispersive spectrometer and a HITACHI S-4800 field emission scanning electron microscope. The EDS spectrum was measured during the TEM measurements. Raman spectra were recorded on an inVia Raman microprobe (Renishaw Instruments, England) with 514 nm laser excitation.

### 2.3. Preparation of graphene

Graphene sheets tend to form irreversible agglomerates or even restack to form graphite through van der Waals interactions because they have a high specific surface area [28]. As most of the unique properties are only associated with their individual sheets, graphene sheets must be well separated from each other using a few methods like protection with special molecules or groups. Herein, we prepared sulfonated graphene (GS) according to the literature with a little modification [29]. Graphite oxide (GO), prepared from natural graphite flakes by a modified Hummer's method [30,31], was used as the starting material to prepare sulfonated graphene. In a typical procedure, 75 mg of graphite oxide was dispersed in 75 g of water. After sonication for 45 min, a clear, brown dispersion of graphene oxide was formed. Then, 600 mg of sodium borohydride in 15 g of water was added into the dispersion of graphene oxide after its pH was adjusted to 9–10 with 5 wt.% sodium carbonate solution. The mixture was then kept at 80 °C for 1 h under constant stirring. After filtering and washing with water using a 0.2 μm Nylon Millipore filter, the partially reduced graphene oxide could be redispersed in 75 g of water via mild sonication. The aryl diazonium salt used for sulfonation was prepared from the reaction of 46 mg of sulfanilic acid and 18 mg of sodium nitrite in 10 g of water and 0.5 g of 1 M HCl solution in an ice bath. The diazonium salt solution was added to the dispersion of partially reduced graphene oxide in a cryostat (0 °C) under stirring. The mixture was kept in the cryostat for 2 h. After filtering and washing with water, sulfonated graphene oxide was redispersed in 75 g of water. In the final reduction step, 2 g of hydrazine in 5 g of water was added into the dispersion and the reaction mixture was kept at 100 °C for 24 h under constant stirring. After filtering and washing with water thoroughly, the graphene thus prepared was readily dispersed in water via a few minutes of sonication.

### 2.4. Preparation of biosensor

Prior to modification, GCE was carefully polished with 1.0 μm, 0.3 μm and 0.05 μm α-alumina powders in sequence, rinsed thoroughly with pure water between each polishing step, sonicated in ethanol and pure water for 5 min respectively and dried with nitrogen. Graphene was dispersed in 0.5% CS acetic acid solution with a few minutes of ultrasonication to achieve a 0.5 mg/mL concentration (GS–CS). After the pH of GS–CS was adjusted above 5 by 1 M NaOH, 20 μL of GS–CS and 10 μL of HRP solution (10 mg/mL) were mixed adequately. Then 8 μL of the mixture (HRP/GS/CS) was cast onto the surface of the GCE. After being dried in refrigerator at 4 °C, the electrode was immersed into a 0.2 M $Na_2SO_4$ solution containing 1 mM $HAuCl_4$. Electrodeposition of Au was carried out under −0.2 V for 300 s, followed by gentle washing in water and drying in a refrigerator. For comparison, HRP/CS/GCE, Au/HRP/CS/GCE and GS/HRP/CS/GCE were prepared with a similar method.

## 3. Results and discussion

### 3.1. Characterization of graphene oxide and graphene

In order to avoid the agglomeration of graphene sheets, we introduced a small number of p-phenyl-$SO_3H$ groups into the product before it was finally reduced by hydrazine. The presence of

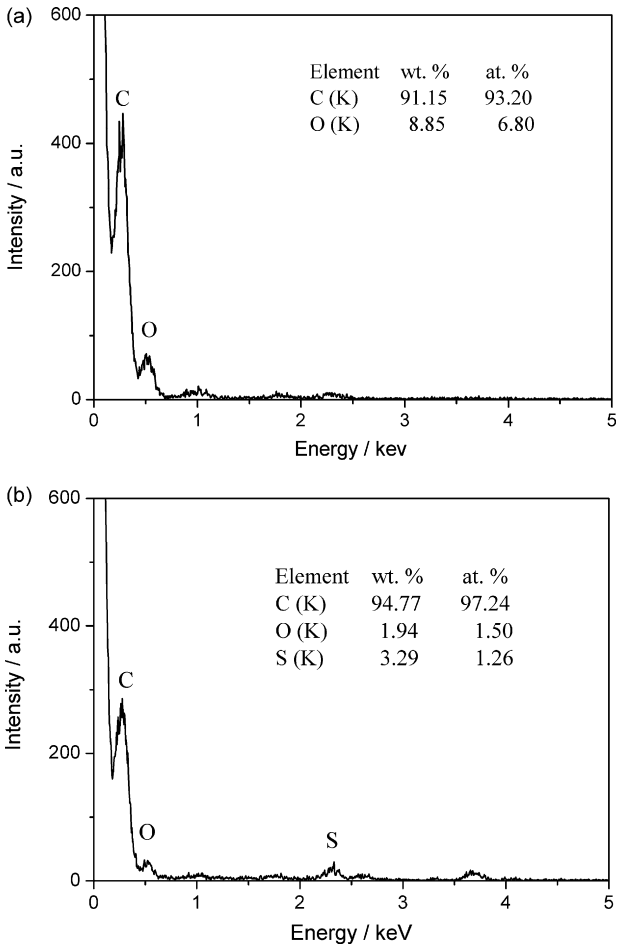


**Fig. 1.** EDS spectra of graphite oxide (a) and graphene (b).

negatively charged $-SO_3^-$ kept the graphene sheets separate due to electrostatic repulsion. Fig. 1 shows the EDS spectra of graphite oxide (a) and graphene (b). Compare to GO, the O content of graphene decreased markedly while the S element emerged, which indicates that most of the oxygen functionalities contain –OH, –O– and –COOH of graphite oxide were removed after reduction, and $-SO_3^-$ was successfully imported.

Raman scattering, which is often used to monitor the structural changes of carbon materials, provided additional evidence of graphene herein. As Fig. 2a shows, pristine graphite displays a prominent peak at 1582 $cm^{-1}$ known as the G band, which corresponds to the first-order scattering of the $E_{2g}$ mode [32]. The Raman spectrum of GO has two prominent peaks at 1602 $cm^{-1}$ and 1349 $cm^{-1}$, corresponding to the well documented G and D bands respectively. The G band broadened compared to pristine graphite, mainly due to the extensive oxidation. After being reduced by hydrazine, the Raman spectrum of graphene also contained both G and D bands (1592 $cm^{-1}$ and 1353 $cm^{-1}$). However, the D/G intensity ratio increased in comparison with GO. Results obtained in this study agree well with former research [33,34], indicating that GO has been well deoxygenated into graphene.

A TEM image of graphene is shown in Fig. 3, clearly illustrating that the transparent sheets are flake-like with wrinkles, which may be the key point leading to a gain in elastic energy for the quasi-two dimension crystallite to avoid dislocations caused by thermal fluctuations and keep a metastable state [35]. The TEM result indicates that the reduction and sulfonation procedures did not cause the morphology of graphene to become damaged. As most unique properties of graphene are dependent on its individual sheet structure, the preservation of the morphology may be important to the performance of graphene in as-prepared biosensors.

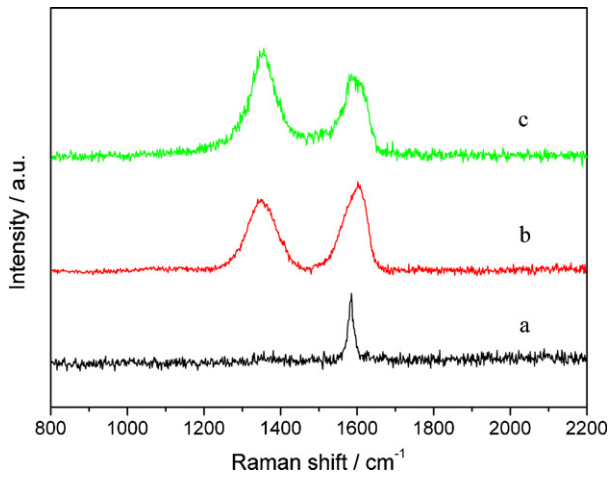


**Fig. 2.** Raman spectra of pristine graphite (a), GO (b) and GS (c).

### 3.2. Electrodeposition of Au on HRP/GS/CS/GCE

Chitosan is a polysaccharide from the deacetylation of chitin. It is positively charged when pH < 6.3 due to the protonation of amino groups, and thus chitosan can electrostatically bind negatively charged $AuCl_4^-$ [36]. Under potentiostatic conditions, Au nanoparticles can grow gradually on the surface of the electrode modified with chitosan. Fig. 4 is the SEM image of the Au/HRP/GS/CS modified electrode. It can be seen from the image that the Au nanoparticles tend to form flower-liked clusters. The inset is a magnification of a cluster, which shows that the diameter of one single Au nanoparticle ranges from 30 nm to 40 nm.

### 3.3. Electrochemical behaviors of the biosensor

Fig. 5 shows the cyclic voltammograms (CVs) of the HRP/CS/GCE (a), Au/HRP/CS/GCE (b), GS/HRP/CS/GCE (c) and Au/GS/HRP/CS/GCE (d) in 0.1 M PBS (pH = 6.5) with a scan rate of 100 mV $s^{-1}$. There is no redox peak current of HRP on the HRP/CS/GCE. This can be

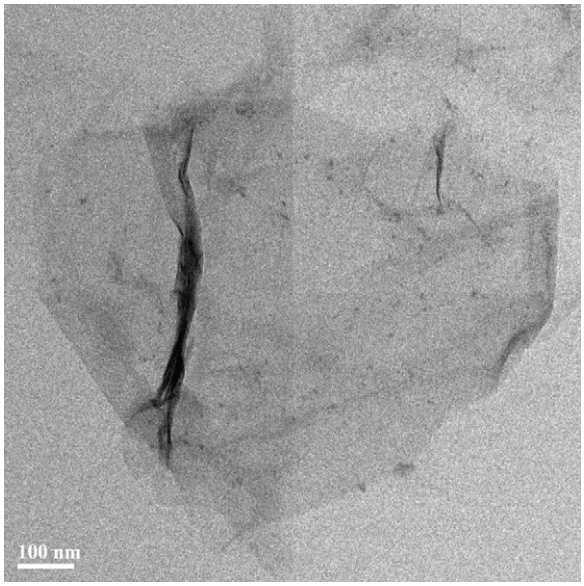


**Fig. 3.** TEM image of graphene.

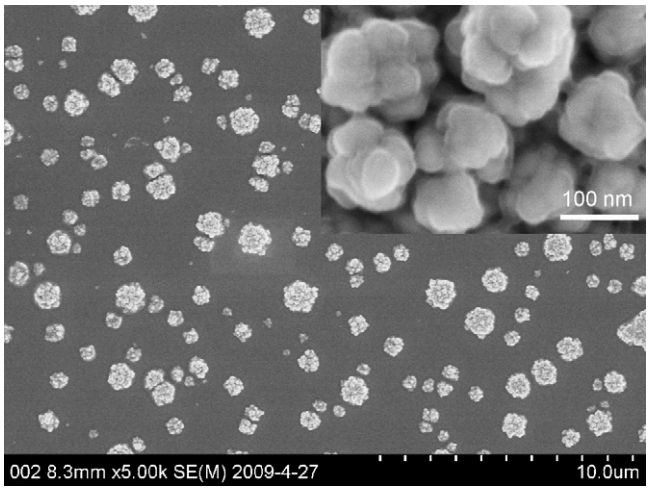


**Fig. 4.** SEM image of Au/HRP/GS/CS modified electrode. The insert shows a cluster of Au nanoparticles.

explained by the deep embedding of the redox center of HRP in a protein shell, which makes the distance between the active site of enzyme and electrode farther than the distance that electrons can transfer at a sufficient rate. The insulation of the biopolymer chitosan further interrupts the electron transfer. In contrast, the Au/HRP/CS/GCE and GS/HRP/CS/GCE both display a prominent cathodic peak current around −0.3 V, suggesting that direct electron transfer was realized. The Au/GS/HRP/CS/GCE shows the largest cathodic peak current compared to the other electrodes. As we know, in an enzyme molecule, the rate coefficient of electron transfer between the donator and acceptor decreases exponentially with the distance between electron transfer centers [37]. After graphene and Au nanoparticles were introduced, the distance between the active site and the microelectrodes was much smaller than the original distance between the enzyme and the electrode surface. The nanoscale individual sheets and particles both act as "molecular wires" to connect the active sites with the electrode, increasing the electron transfer rate significantly. In addition, the high conductivity of graphene is also responsible for the increased current. Electrons can travel without being scattered off course by lattice imperfections and foreign atoms in graphene due to the high quality of its crystal lattice. The conduction electrons of graphene move much faster and as if they had far less mass than the electrons

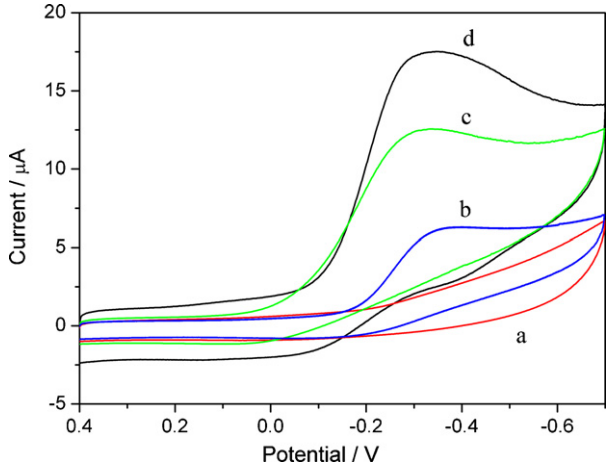


**Fig. 5.** Cyclic voltammograms of HRP/CS/GCE (curve a), Au/HRP/CS/GCE (curve b), GS/HRP/CS/GCE (curve c) and Au/GS/HRP/CS/GCE (curve d) in 0.1 M PBS (pH 6.5) at a scan rate of 0.1 V $s^{-1}$.

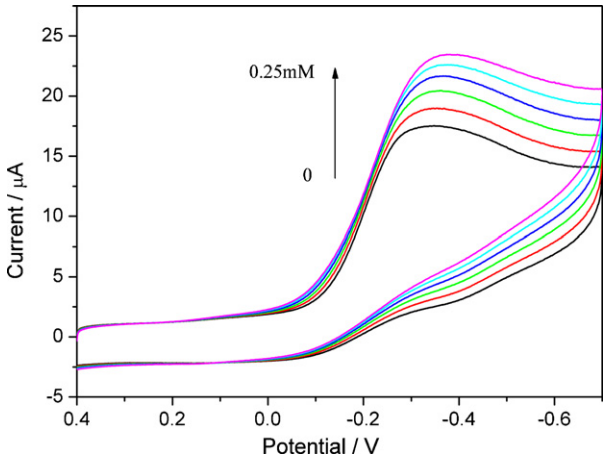


**Fig. 6.** Cyclic voltammograms of Au/GS/HRP/CS/GCE with successive addition of 0.05 mM $H_2O_2$ in 0.1 M PBS at pH 6.5 at a scan rate of 0.1 V $s^{-1}$.

that wander about through ordinary metals and semiconductors [38]. These two factors mentioned above make electron transfer in the composite possible.

The CVs of Au/GS/HRP/CS/GCE in different concentrations of $H_2O_2$ were also investigated. As shown in Fig. 6, the cathodic peak current increased dramatically upon the addition of $H_2O_2$, which is a typical representation of the catalytic reduction of $H_2O_2$. The catalytic mechanism of the immobilized HRP to $H_2O_2$ can be explained by the following scheme [39]:

$$HRP(Fe^{3+}) + H_2O_2 \rightarrow CompoundI(Fe^{4+}{=}O) + H_2O \quad (1)$$

$$CompoundI(Fe^{4+}{=}O) + e^- + H^+ \rightarrow CompoundII \quad (2)$$

$$CompoundII + e^- + H^+ \rightarrow HRP(Fe^{3+}) + H_2O \quad (3)$$

HRP reacts with $H_2O_2$ to form a first intermediate (Compound I), which is a two-equivalent oxidized form containing an oxyferryl heme ($Fe^{4+}$=O) and a porphyrin π cation radical. Compound I show catalytic activity, and its porphyrin radical abstracts one electron from the electrode to form a second intermediate (Compound II), which is subsequently reduced back to the native HRP by accepting one electron from the electrode [39].

The pH value of the electrolyte is important for the performance of the biosensor because the activity of the enzyme is affected greatly by pH. Fig. 7 shows the amperometric response of Au/GS/HRP/CS/GCE at different pH values with the presence of the same concentration of $H_2O_2$. As can be seen, the response current

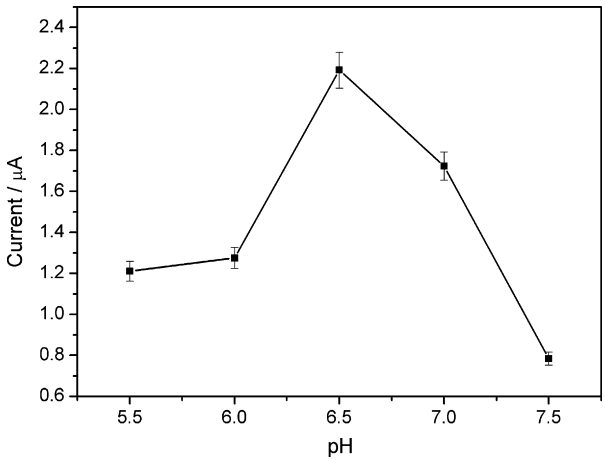


**Fig. 7.** Effect of pH on the performance of Au/GS/HRP/CS/GCE in the presence of the same concentration of $H_2O_2$ in 0.1 M PBS at potential of −0.3 V.

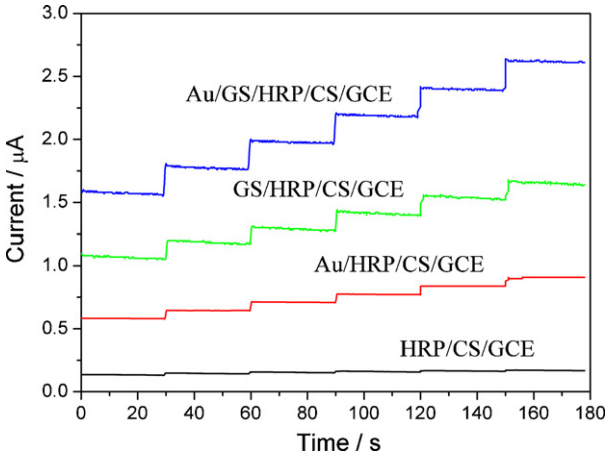


**Fig. 8.** Current response to successive addition of 0.2 mM $H_2O_2$ of HRP/CS/GCE, Au/HRP/CS/GCE, GS/HRP/CS/GCE and Au/GS/HRP/CS/GCE in 0.1 mol $L^{-1}$ PBS (pH 6.5). Operating potential: −0.3 V.

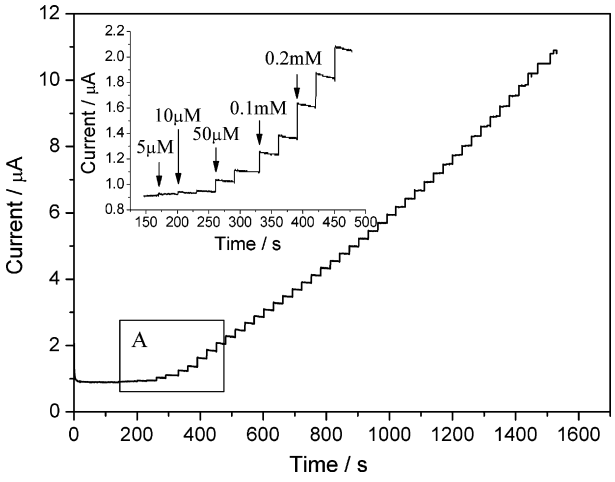


**Fig. 9.** Current–time response of Au/GS/HRP/CS/GCE for successive addition of $H_2O_2$ in 0.1 M PBS (pH 6.5). Inset: amplification of part A. Operating potential: −0.3 V.

increased from pH 5.5 and reached the maximum at pH 6.5, then decreased to pH 7.5. Strongly acidic or alkaline environments would result in the denaturation of enzyme; however, a faintly acidic solution enhances the reaction because $H^+$ is needed for HRP to reduce the $H_2O_2$ and produce water [40]. Therefore, pH 6.5 is selected as the optimized value for the HRP, in agreement with the report that HRP is entrapped in a CS matrix [41].

To comprehend the role of graphene in biosensors, four different electrodes were prepared, and their current responses to the same concentration of $H_2O_2$ were studied. As Fig. 8 shows, HRP/CS/GCE only yielded a negligible current response to the addition of 0.2 mM $H_2O_2$, indicating that the direct electron transfer between the HRP and the electrode is difficult. A slight increase of current is observed in Au/HRP/CS/GCE compared to HRP/CS/GCE mostly due to the introduction of Au. The GS/HRP/CS/GCE caused an obvious increase in current, and when graphene was combined with Au, a relatively high current response, which was 3 times larger than Au/HRP/CS/GCE and almost 20 times larger than HRP/CS/GCE, was observed. The different performances of electrodes are mainly attributed to the excellent properties of graphene. These carbon-based individual sheets have good electrocatalytic activity towards $H_2O_2$, and the high surface area-to-volume ratio is favorable for enzyme immobilization. The eximious electronic conductivity benefits the direct electrons transfer between the enzyme and electrode, and furthermore, the good biocompatibility is good for HRP to maintain bioactivity. The response current of Au/GS/HRP/CS/GCE is larger than the summation of Au/HRP/CS/GCE and GS/HRP/CS/GCE, distinctly illuminating the synergistic effect of the Au–graphene composite.

The typical current–time plot of Au/GS/HRP/CS/GCE with successive injection of $H_2O_2$ is given in Fig. 9. The working potential was set at −0.3 V, where the amperometric response reached the maximum value, as Fig. 5 shows. The biosensor responded rapidly

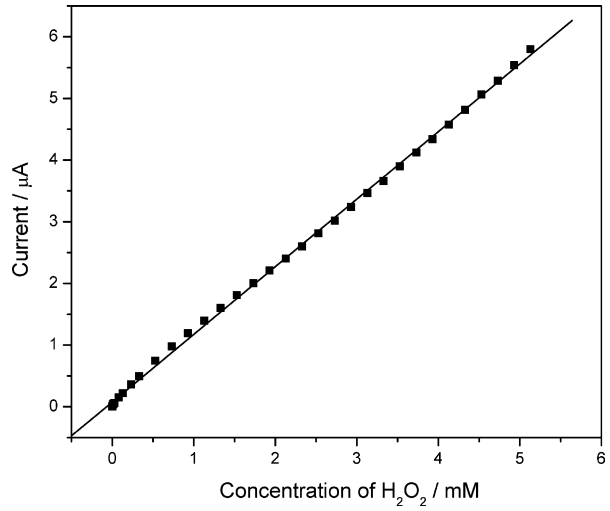


**Fig. 10.** Calibration curve between current and the concentration of $H_2O_2$. pH of 0.1 M PBS: 6.5. Operating potential: −0.3 V.

when $H_2O_2$ was added and reached a steady state (95% of the maximum value) within 3 s, indicating a fast diffusion of the substrate in the hybrid film modified on the electrode and the high sensitivity of the biosensor. Fig. 10 shows the calibration curve of the amperometric response. The biosensor has a good linear relationship with $H_2O_2$ in the range from $5 \times 10^{-6}$ M to $5.13 \times 10^{-3}$ M with a correlation coefficient of 0.999, which is much wider than some other hydrogen peroxide biosensors based on HRP [42–44]. The detection limit was estimated to be $1.7 \times 10^{-6}$ M at a signal-to-noise ratio of 3. The Michaelis–Menten constant ($K_m$), which is a reflection of both the enzymatic affinity and the ratio of microscopic kinetic constant, was calculated to be 2.61 mM according to the Lineweaver–Burk

**Table 1**
Comparison of the proposed $H_2O_2$ biosensor with other biosensors based on HRP.

| $H_2O_2$ biosensor | Operating potential (V) | Linear range (mM) | Detection limit (μM) | $K_m$ value (mM) | Reference |
|---|---|---|---|---|---|
| Au/GS/HRP/CS | −0.3 | 0.005–5.13 | 1.7 | 2.61 | Present work |
| ZnO/GNPs/Nafion/HRP | −0.3 | 0.015–1.1 | 9 | 1.76 | [46] |
| Clay/HRP/Au/CS | −0.3 | 0.039–4.1 | 9 | 23.15 | [47] |
| HRP/$Fe_3O_4$/CS | −0.2 | 0.2–12 | 100 | 21.4 | [48] |
| Au/CS/HRP | −0.3 | 0.012–2.43 | 6.3 | 0.36 | [49] |
| HRP/Nafion/Sonogel/Carbon | −0.25 | 0.004–0.1 | 1.6 | 0.295 | [50] |
| CMCS/Au/HRP | −0.4 | 0.005–1.4 | 0.401 | 0.57 | [51] |

GNPs: gold nanoparticles; CMCS: carboxymethyl chitosan.

equation [45]. The further comparison of Au/GS/HRP/CS/GCE developed in this study with other biosensors based on HRP is shown in Table 1.

### 3.4. Stability and reproducibility of the biosensor

The long-term stability of our fabricated biosensor was investigated by examining its current response during storage in a refrigerator at 4 °C. The biosensor exhibited no obvious decrease in current response in the first week and maintained about 92% of its initial value after 3 weeks. The repeatability of the measurement was obtained by detecting 0.05 mM $H_2O_2$ 10 times using the same electrode. The relative standard deviation (R.S.D.) was found to be 3.6%. Five electrodes were prepared utilizing the same method to check the reproducibility of the biosensor. To detect the same concentration of $H_2O_2$ of 0.05 mM, the result revealed a R.S.D. of 4.2%, which is acceptable.

## 4. Conclusion

In this paper, individual graphene sheets were successfully prepared by the introduction of $-SO_3^-$. EDS and TEM indicated that the reduction and sulfonation procedures did not cause the morphology of graphene to be damaged, which is important for the maintenance of the excellent properties of graphene. The as-prepared graphene was combined with CS, Au and HRP to construct a $H_2O_2$ biosensor. Cyclic voltammograms showed that the biosensor realized the direct electron transfer between HRP and the electrode and exhibited the typical catalytic reduction of $H_2O_2$. The comparison of the current response to the same concentration of $H_2O_2$ of HRP/CS/GCE, Au/HRP/CS/GCE, GS/HRP/CS/GCE and Au/GS/HRP/CS/GCE demonstrated that graphene can greatly improve the sensitivity of the biosensor. In addition, the biosensor reveals some other excellent characteristics such as wide linear range, low detection limit and long-term stability. In summary, the biosensor with easy fabrication, low cost and good performance proposed in this paper provides a new strategy for the construction of $H_2O_2$ biosensors and can be applied in practice.

## Acknowledgments

This work was supported by the National Natural Science Foundation of China (20676038 and 20976054), the Key Project of Science and Technology for Ministry of Education (107045), the Innovation Program of Shanghai Municipal Education Commission (09ZZ58), the Program of Shanghai Subject Chief Scientist (08XD1401500), the Shuguang Scholar-Tracking Foundation of Shanghai (08GG09), and the Shanghai Leading Academic Discipline Project (B502).

## References

[1] A.K. Geim, A.H. MacDonald, Phys. Today 60 (2007) 35.
[2] H. Chen, M.B. Müller, K.J. Gilmore, G.G. Wallace, D. Li, Adv. Mater. 20 (2008) 3557.
[3] S. Stankovich, D.A. Dikin, G.H.B. Dommett, K.M. Kohlhaas, E.J. Zimney, E.A. Stach, R.D. Piner, S.T. Nguyen, R.S. Ruoff, Nature 442 (2006) 282.
[4] S. Gilje, S. Han, M.S. Wang, K.L. Wang, R.B. Kaner, Nano Lett. 7 (2007) 3394.
[5] J.S. Bunch, Z.A.M. Vander, S.S. Verbridge, I.W. Frank, D.M. Tanenbaum, J.M. Parpia, H.G. Craighead, P.L. McEuenh, Science 315 (2007) 490.
[6] J.B. Wu, H.A. Becerril, Z.A. Bao, Z.F. Liu, Y.S. Chen, P. Peter, Appl. Phys. Lett. 92 (2008) 263302.
[7] C.S. Shan, H.F. Yang, J.F. Song, D.X. Han, A. Ivaska, L. Niu, Anal. Chem. 81 (2009) 2378.
[8] Y. Wang, Y.M. Li, L.H. Tang, J. Lu, J.H. Li, Electrochem. Commun. 11 (2009) 889.
[9] X.L. Luo, J.J. Xu, W. Zhao, H.Y. Chen, Biosens. Bioelectron. 19 (2004) 1295.
[10] X. Cui, G. Liu, Y. Lin, J. Biomed. Nanotechnol. 1 (2005) 1.
[11] X.B. Lu, J.H. Zhou, W. Lu, Q. Liu, J.H. Li, Biosens. Bioelectron. 23 (2008) 1236.
[12] X.H. Shu, Y. Chen, H.Y. Yuan, S.F. Gao, D. Xiao, Anal. Chem. 79 (2007) 3695.
[13] N.V. Klassen, D. Marchington, H.C.E. McGovan, Anal. Chem. 66 (1994) 2921.
[14] M.C.Y. Chang, A. Pralle, E.Y. Isacoff, C.J. Chang, J. Am. Chem. Soc. 126 (2004) 15392.
[15] C. Matsubara, N. Kawamoto, K. Takamura, Analyst 117 (1992) 1781.
[16] D.W. King, W.J. Cooper, S.A. Rusak, B.M. Peake, J.J. Kiddle, D.W. O'Sullivan, M.L. Melamed, C.R. Morgan, S.M. Theberge, Anal. Chem. 79 (2007) 4169.
[17] J.B. Jia, B.Q. Wang, A.G. Wu, G.J. Cheng, Z. Li, S.J. Dong, Anal. Chem. 74 (2002) 2217.
[18] X.L. Luo, J.J. Xu, Q. Zhang, G.J. Yang, H.Y. Chen, Biosens. Bioelectron. 21 (2005) 190.
[19] B. Wang, J.J. Zhang, Z.Y. Pan, X.Q. Tao, H.S. Wang, Biosens. Bioelectron. 24 (2009) 1141.
[20] W. Zhang, G.F. Wang, X.J. Zhang, B. Fang, Electroanalysis 21 (2009) 179.
[21] J. Pillay, K.I. Ozoemena, Electrochim. Acta 54 (2009) 5053.
[22] Salimia, R.G. Comptonb, R. Hallaja, Anal. Biochem. 333 (2004) 49.
[23] J.J. Gooding, R. Wibowo, J.Q. Liu, W.R. Yang, D. Losic, S. Orbons, F.J. Mearns, J.G. Shapter, D.B. Hibbert, J. Am. Chem. Soc. 125 (2003) 9006.
[24] J. Wang, Electroanalysis 17 (2005) 7.
[25] P. Sorlier, A. Denuziere, C. Viton, A. Domard, Biomacromolecules 2 (2001) 765.
[26] Y.L. Yao, K.K. Shiu, Electroanalysis 20 (2008) 1542.
[27] Y.L. Yao, Y. Ding, L.S. Ye, X.H. Xia, Carbon 44 (2006) 61.
[28] D. Li, M.B. Müller, S. Gilje, R.B. Kaner, G.G. Wallace, Nat. Nanotechnol. 3 (2008) 101.
[29] Y.C. Si, E.T. Samulski, Nano Lett. 8 (2008) 1679.
[30] W.S. Hummers, R.E. Offeman, J. Am. Chem. Soc. 80 (1958) 1339.
[31] N.I. Kovtyukhova, P.J. Ollivier, B.R. Martin, T.E. Mallouk, S.A. Chizhik, E.V. Buzaneva, A.D. Gorchinskiy, Chem. Mater. 11 (1999) 771.
[32] F. Tuinstra, J.L. Koenig, J. Chem. Phys. 53 (1970) 1126.
[33] S. Stankovich, D.A. Dikin, R.D. Piner, K.A. Kohlhaas, A. Kleinhammes, Y. Jia, Y. Wu, S.T. Nguyen, R.S. Ruoff, Carbon 45 (2007) 1558.
[34] Y.X. Xu, H. Bai, G.W. Lu, C. Li, G.Q. Shi, J. Am. Chem. Soc. 130 (2008) 5856.
[35] A.K. Geim, K.S. Novoselov, Nat. Mater. 6 (2007) 183.
[36] X.H. Kang, Z.B. Mai, X.Y. Zou, P.X. Cai, J.Y. Mo, Anal. Biochem. 369 (2007) 71.
[37] X.L. Ren, X.W. Meng, D. Chen, F.Q. Tang, J. Jiao, Biosens. Bioelectron. 21 (2005) 433.
[38] A.K. Geim, P. Kim, Sci. Am. 4 (2008) 90.
[39] Y. Xiao, H.X. Ju, H.Y. Chen, Anal. Biochem. 278 (2000) 22.
[40] T. Tangkuaram, C. Ponchio, T. Kangkasomboon, P. Katikawong, W. Veerasai, Biosens. Bioelectron. 22 (2007) 2071.
[41] F.N. Xi, L.J. Liu, Q. Wu, X.F. Lin, Biosens. Bioelectron. 24 (2008) 29.
[42] J.W. Wang, L.P. Wang, J.W. Di, Y.F. Tu, Talanta 77 (2009) 1454.
[43] C.X. Lei, H. Wang, G.L. Shen, R.Q. Yu, Electroanalysis 16 (2004) 736.
[44] A.K.M. Kafi, G.S. Wu, A.C. Chen, Biosens. Bioelectron. 24 (2008) 566.
[45] R.A. Kamin, G.S. Willson, Anal. Chem. 52 (1980) 1198.
[46] C.L. Xiang, Y.J. Zou, L.X. Sun, F. Xu, Sens. Actuators B 136 (2009) 158.
[47] X.J. Zhao, Z.B. Mai, X.H. Kang, X.Y. Zou, Biosens. Bioelectron. 23 (2008) 1032.
[48] X.C. Tan, J.L. Zhang, S.W. Tan, D.D. Zhao, Z.W. Huang, Y. Mi, Z.Y. Huang, Electroanalysis 21 (2009) 1514.
[49] C.X. Lei, S.Q. Hu, G.L. Shen, R.Q. Yu, Talanta 59 (2003) 981.
[50] M. Elkaoutit, I. Naranjo-Rodriguez, M. Dominguez, M.P. Hernandez-Artiga, D. Bellida-Milla, J.L.H.H. de Cisneros, Electrochim. Acta 53 (2008) 7131.
[51] Q. Xu, C. Mao, N.N. Liu, J.J. Zhu, J. Sheng, Biosens. Bioelectron. 22 (2006) 768.